Electronic Supplementary Information

Innovative design of bismuth-telluride-based thermoelectric micro-generators with high output power

S. El Oualid[1], F. Kosior[1], A. Dauscher[1], C. Candolfi[1], G. Span[2], E. Mehmedovic[3], J. Paris[4], B. Lenoir[1,*]

[1] *Institut Jean Lamour, UMR 7198 CNRS – Université de Lorraine, 2 allée André Guinier – Campus ARTEM, BP 50840, 54011, Nancy Cedex, France*

[2] *Mahle Thermoelektronik GmbH, Duisburg, Germany*

[*]Corresponding Author: bertrand.lenoir@univ-lorraine.fr

[+] Present address: *SAM GmbH&CoKG, Himmelreichweg 4, A-6112 Wattens, Austria*

[⊥] Present address: *STAUFFEN.Quality Engineers GmbH, Blumenstraβe 5, D-73257 Köngen, Germany*

Content

Figure S4. Temperature and voltage profiles in the thermocouple calculated by finite-element analyses.

Figure S5. Sketch showing the equivalence between the rectangular-shaped geometry of the thermocouple and that of a linear narrow band.

Figure S6. Maximum output power P_{max} as a function of m or $(a + b)$ calculated using COMSOL.

Figure S7. Plots showing the electrical and thermal boundary conditions.

Figure S8. Maximum output power and temperature difference between the hot and cold side as a function of the heat exchange coefficient h_{ex}.

Figure S9. Calculated output power as a function of the parameter s for fixed boundary conditions with and without the presence of the ENIG diffusion barrier.

Table S3. Optimized geometrical parameters of the μ-TEG.

Group based on	Team/Company	μ-TEG design and fabrication							TE materials		Characteristics of the μ-TEG					References
		Configuration	Leg length (μm)	Leg area (μm²)	Number of thermocouples	A_d (mm²)	Technology/Substrate	Filling rate (10^{-5})			Electrical resistance (kΩ)	ΔT applied (K)	Voc @ ΔT (V)	Power @ ΔT (μW)	Normalized power (μW/cm²K²)	
Si-based materials	UT	Cross-plane	0.35	~0.06	~72	1.73×10^{-3}	CMOS-MEMS/Si	~500	p-Si	n-Si	9×10^{-3}	33.9	~0.0046	0.6	29	29
	Infineon	In plane/lateral	18.5	6×0.4	15872	7	CMOS-MEMS/Si	1088	p-Si	n-Si	2100	5	~0.8	~0.08	0.043	30
	IMEC	Cross-plane	-	~3×3	~4700	16	MEMS/Si	~528	p-SiGe	n-SiGe	~4000	1	0.25	$\sim4.1\times10^{-3}$	0.026	31
	UW	In-plane/lateral	4500	100×0.4	5	~0.8	MEMS/Saphir	50	p-Si	n-Si	69	11	0.024	0.002	2.1×10^{-3}	32
	HSG-IMIT	In-plane/ lateral	500	7×1.2	1000	~22	MEMS/Si	76	Al	n-Si	900	10	2.4	1.5	~0.068	33
Semiconductors materials	Micropelt	Cross-plane	500	35×35	1132	25	MEMS-sputtering/Si	11094	n,p $(Bi,Sb)_2(Te,Se)_3$		0.236	15	3.5	6000	106.6	34
	JPL	Cross-plane	20	2826	63	2.5	MEMS-Electrodeposition/Si	14243	p-$Bi_{2-x}Sb_xTe_3$	n-Bi_2Te_3	12×10^{-3} – 30×10^{-3}	–	0.004	1	-	35
	Komatsu	In plane/lateral	15000	1000×1	7	~24	Flash evaporation/Glass	58	p-$Bi_{0.4}Sb_{1.6}Te_3$	n-$Bi_2Te_{2.7}Se_{0.3}$	8.5	30	0.083	0.21	$\sim97\times10^{-5}$	36
	UY	In plane/ vertical	20000	670×4	300	1200	Flash evaporation/Glass	134	p-$Bi_{0.5}Sb_{1.5}Te_3$	n-$Bi_2Te_{2.4}$ $Se_{0.6}$	89	40	4	45	0.0023	37
	Seiko	Cross-plane	600	80×80	52	~ 1.9	Hot pressing/Si	39153	p-(Bi,SbTe)	n-Bi_2Te_3	0.1	1	0.03	2.25	~115	38
	UF	Cross-plane	80~135	70650	71	96	MEMS-Electrodeposition/Si	10450	p-Sb_XTe_Y /Cu	n-Bi_2Te_3	~0.0038	39	~0.230	2338	1.63	39
	UHK	Cross-plane	10	31.4×10^3	127	32.5	MEMS-Electrodeposition/Si	24540	p-Sb_2Te_3	n-Bi_2Te_3	13×10^{-3}	52.5	0.41	2990	3.34	40
	ETH	Cross-plane	120	34618	99	~22	MEMS-Electrodeposition/Polyimide	15586	p,n-$Bi_{2+x}Te_{3+x}$		-	51.2	-	165	0.288	27
	UC	In plane/vertical	5000	640×90	50	~123	Printing/Polyimide	4683	p-Sb_2Te_3	n-Bi_2Te_3	2.55	20	0.34	10.5	2.1×10^{-2}	41
	IMM	In plane/lateral	3000	~97.5×1	2778	~2500	Sputtering/Polyimide	22	p-Sb_2Te_3	n-Bi_2Te_3	2300	5	2.0	~0.43	$\sim6\times10^{-4}$	42
	DTS	In plane/ vertical	1000	50×2.5	2250	64	Sputtering/Polyimide	879	p-$Bi_{0.5}Sb_{1.5}Te_3$	n-$Bi_2Te_{2.7}$ $Se_{0.3}$	1000	5	2.1	1.1	0.068	19
	This work	**In plane/ vertical**	**70**	**0.39×10^6**	**15/120**	**40.75/326**	**Sputtering/Polyimide**	**290000**	**$(Bi_{0.25}Sb_{0.75})_2Te_3$**	**$Bi_2(Te_{0.9}Se_{0.1})_3$**	**0.0011/0.009**	**5**	**0.004/0.06**	**80.9/647.2**	**7.9/38**	**-**
Organic materials	UN	In plane/lateral	2000	9000×1.85	1	~150	Thermal evaporation/Glass	22	p-TTT	n-TCNQ TTT	15	10	1.8×10^{-3}	55E-6	4×10^{-7}	43
	UD	In plane/ vertical	-	-	-	~65.2	Electro spraying/-	-	p-CNTF	n-CNTF	47×10^{-3}	44.4	4.5×10^{-3}	4.5	35×10^{-4}	44
	BNL	In plane/vertical	10000	2667×150	3	~2.4	Floating catalyst chemical vapor deposition/PET	100000	p-SWCN	n-SWCN	12.5×10^{-3}	27.5	0.011	2.5	0.14	45
Metallic material	ETH	Cross-plane	142	34618	69	20	MEMS-Electrodeposition/Polyimide	11943	Cu	Ni	2×10^{-4}	40	-	0.84	2.64×10^{-3}	27
	Tokai Rika	In plane/vertical	3000	~300×0.15	380	~1910	E beam evaporation/Polyimide	1.8	Cu	Ni	6	1	0.006	0.0016	8×10^{-5}	46

Table S1. Overview of the materials, design, fabrication and main characteristics of selected μ-TEGs materials. The data were taken from the given references, or extracted from figures or graphs when it was possible. These last data, considered as estimated, are indicated by the symbol "~". The configuration refers to the description given in Figure S1 below. The leg area corresponds to the area of the TE material perpendicular to the heat flux. A_d corresponds to the area of the device. The filling rate is defined as the ratio of the total area of the TE materials A_{TE} (A_{TE} = 2 × leg area × number of thermocouples) to A_d. The electrical resistance is the total electrical resistance of the fabricated μ-TEG. ΔT is the temperature difference applied to the μ-TEG during the measurement of the output power. V_{oc} is the open voltage of the μ-TEG under ΔT due to the Seebeck effect. P_{max} corresponds to the maximum power achieved under ΔT. The normalized power is defined as the ratio of P_{max} to $A_d \times \Delta T^2$.

Table S2. Physical properties of the *n*- and *p*-type Bi_2Te_3-based thermoelectric materials, the polyimide and the copper plates used in finite-element analyses.

	***n* type**	***p* type**	**Cooper**	**Polyamide**
Electrical conductivity (S m^{-1})	105 000	76 000	5.99×10^8	-
Thermal conductivity (W m^{-1} K^{-1})	0.75	0.75	400	0.15
Heat capacity (J Kg^{-1} K^{-1})	190	190	385	0.904
Density (g cm^{-3})	7.70	7.74	8.96	1420
Seebeck coefficient (μV K^{-1})	-130	210	6.5	-

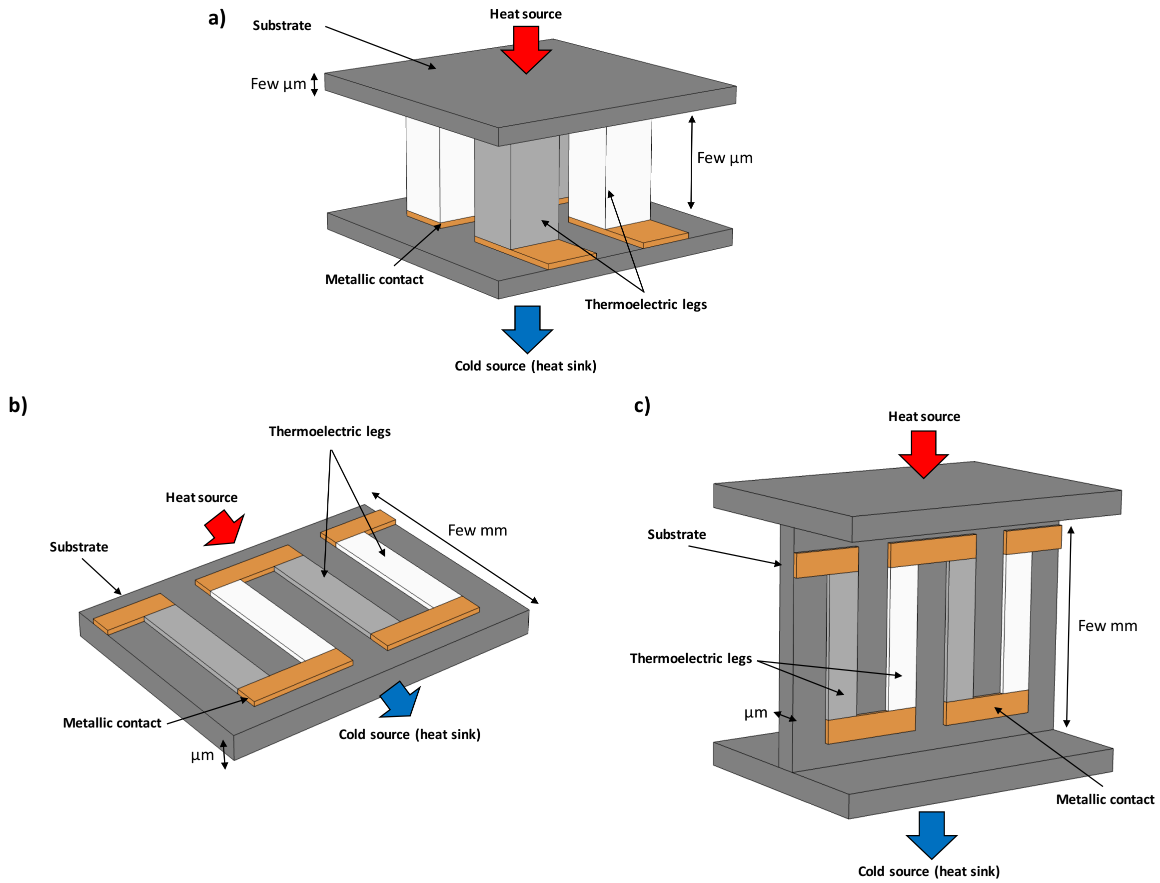

Figure S1. Design of cross-plane and in-plane µ-TEGs. a) The cross-plane architecture is similar to the π-shaped geometry of conventional TEGs in which, the heat flows perpendicularly to the substrate. In this configuration, the length of the *n*- and *p*-type legs are typically on the order of tens to hundreds of µm. In the in-plane configuration, the heat flows parallel to the substrate. There are two principal packaging for this configuration: b) a lateral one (labelled in-plane/lateral) in which the heat flow is parallel to the µ-TEG and c) a vertical one (labelled in-plane/vertical) in which the heat flow is perpendicular through the µ-TEG.

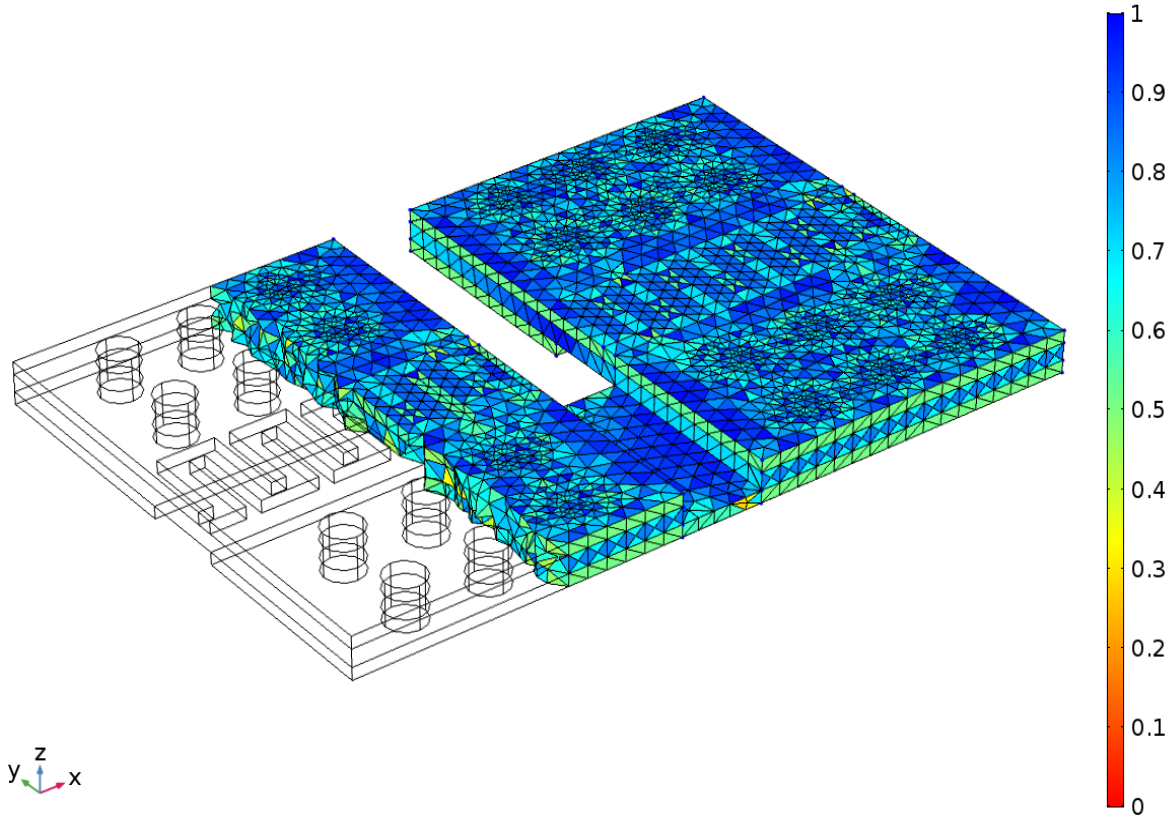

Figure S2. Example of the quality of the meshing considered in our simulations. The left vertical bar shows the asymmetry in volume of the meshing (zero corresponds to a bad quality meshing while a value of one corresponds to a meshing of excellent quality).

a) b)

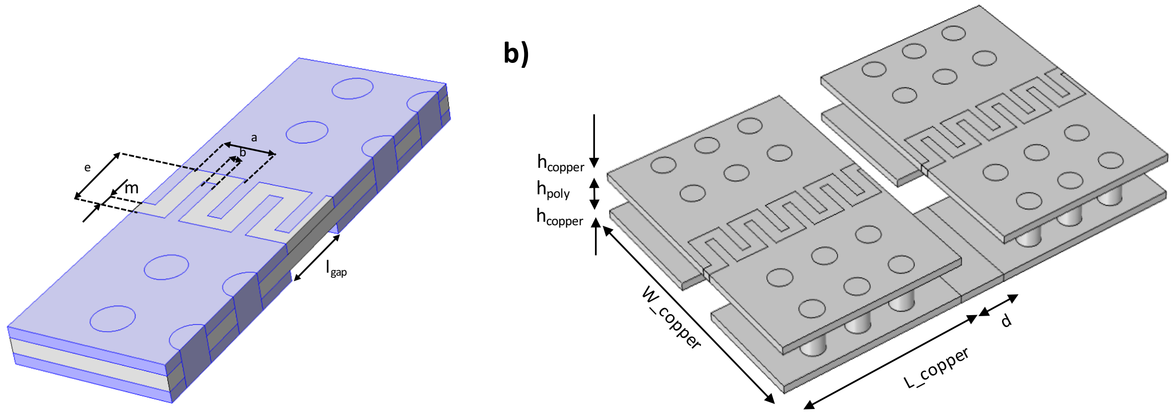

c)

Geometrical parameter	L_cop	W_cop	h_{cop}	h_{poly}	a	b	l_{gap}	m	e	d
Value (mm)	2	3	0.07	0.10	0.34	0.09	0.50	0.05	0.50	0.50

Figure S3. a, b) Definition of the different geometrical parameters of the thermocouple. c) Values considered as a starting point in our simulations.

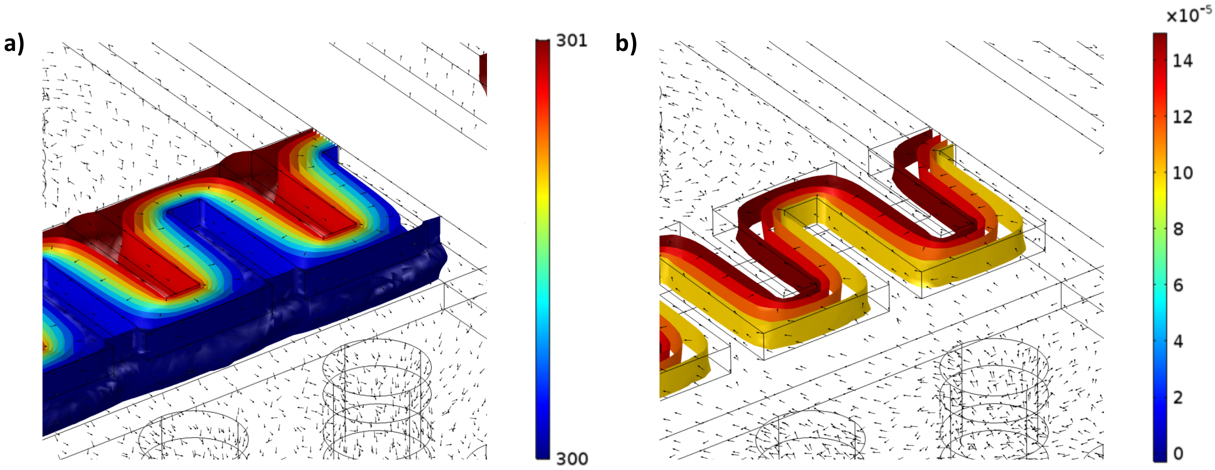

Figure S4. a) Temperature (K, color level) and thermal flux (W m^{-2}, arrows) distributions, b) electrical potential (V, color level) and current density (A m^{-2}, arrows) distributions, calculated for the *n*-type leg under open circuit conditions for ΔT = 1 K.

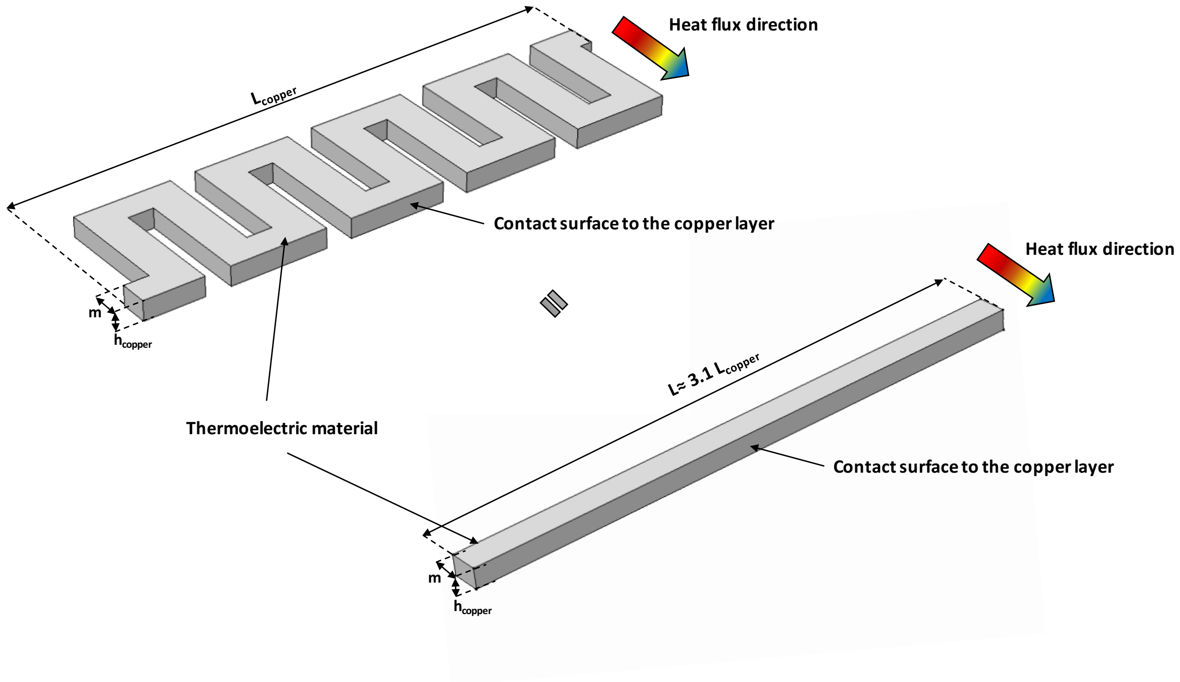

Figure S5. Equivalence between the rectangular-shaped structure and a narrow band of similar total length defined as $L = L_{copper}\left[1 + \frac{2(e-m)}{(a+b)}\right]$. Using the initial values given in Figure S3c, $L \approx 3.1L_{copper}$.

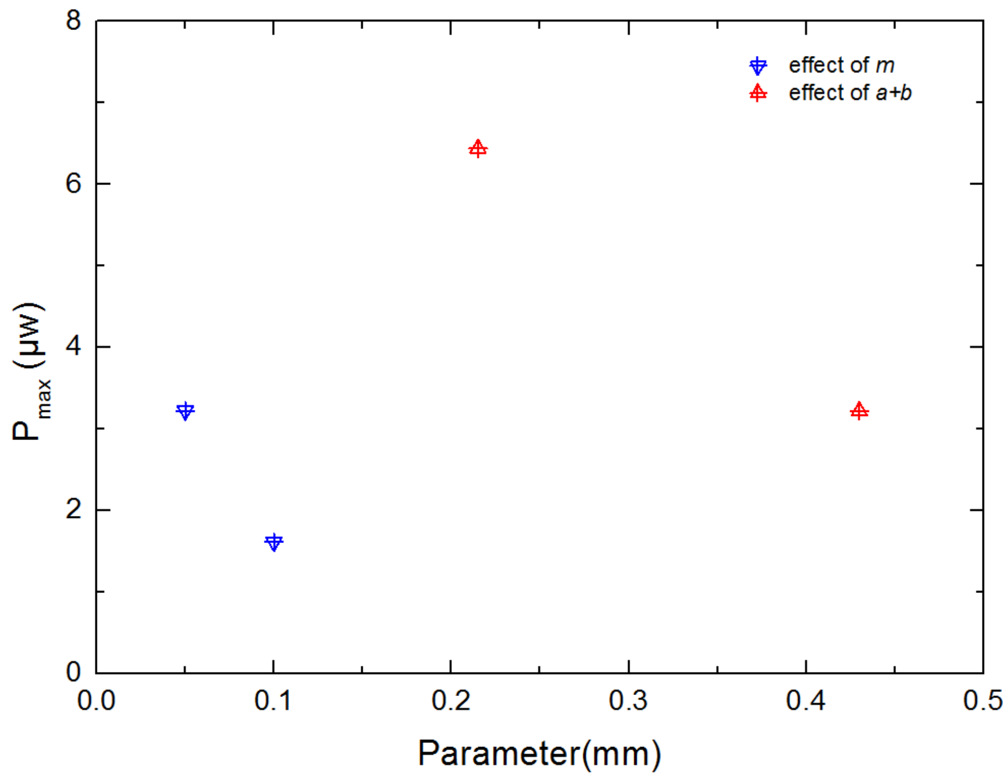

Figure S6. Maximum output power P_{max} as a function of m or $(a + b)$ calculated using COMSOL. The decreases observed in P_{max} with both parameters is in line with Eq.(7).

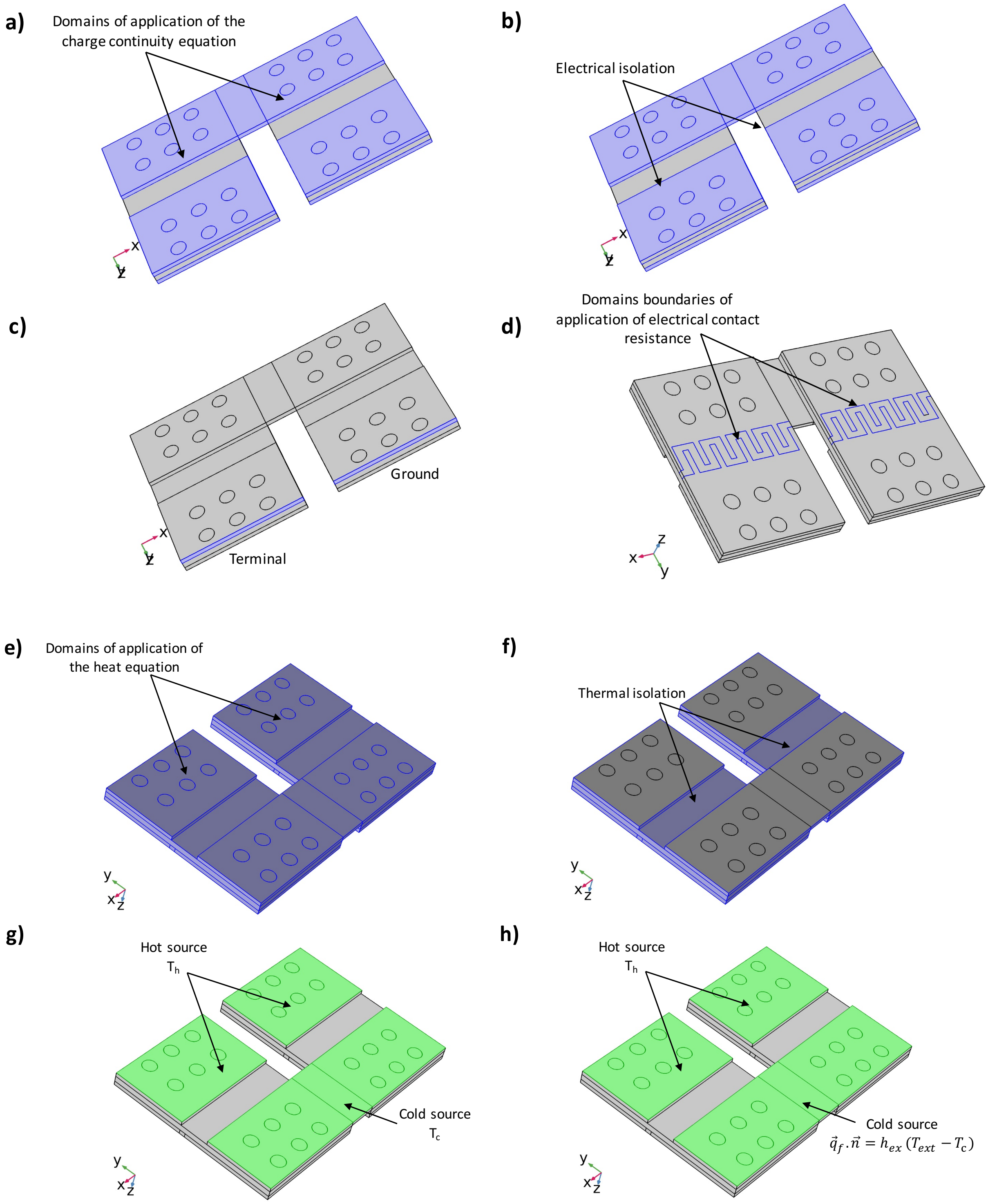

Figure S7. Electrical boundary conditions: a) application domain (parts in purple), b) electrical isolation at the boundaries, c) creation of a terminal and a ground, d) boundary conditions for electrical contact resistance. Thermal boundary conditions: e) application domains (parts in purple), f) thermal isolation at the boundaries, g) fixed temperatures, h) mixed boundary conditions (fixed temperature at the hot side and convective flux at the cold side).

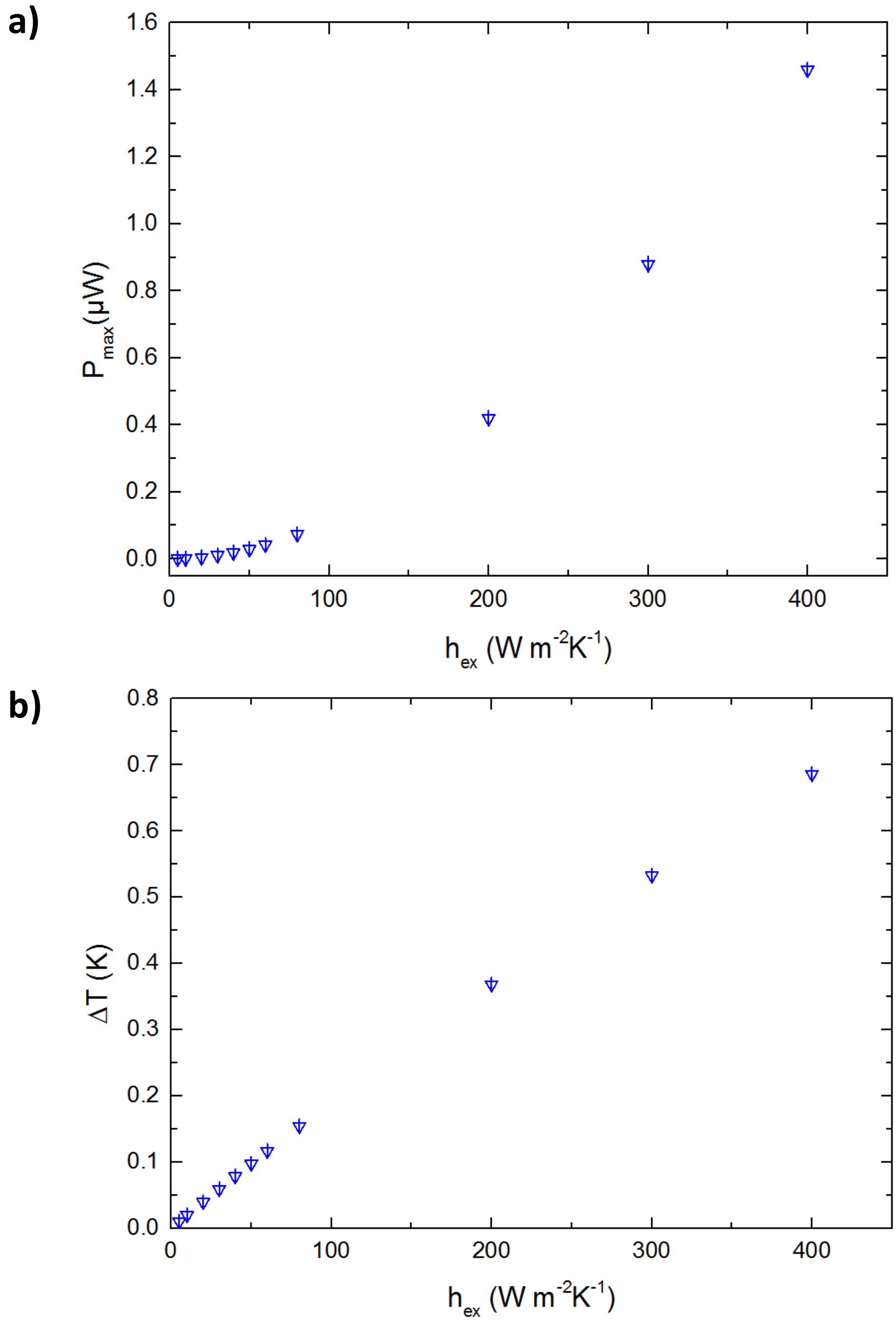

Figure S8. a) Maximum output power P_{max} of the thermocouple as a function of the heat exchange coefficient h_{ex}. b) Temperature difference ΔT between the hot and cold side as a function of the heat exchange coefficient h_{ex}.

Table S3. Optimized geometrical parameters of the μ-TEG.

Geometrical parameter	L_cop	W_cop	h_{cop}	h_{poly}	a	b	l_{gap}	m	e	d
Value (mm)	2	3	0.07	0.10	0.34	0.09	0.50	0.38	0.54	0.50

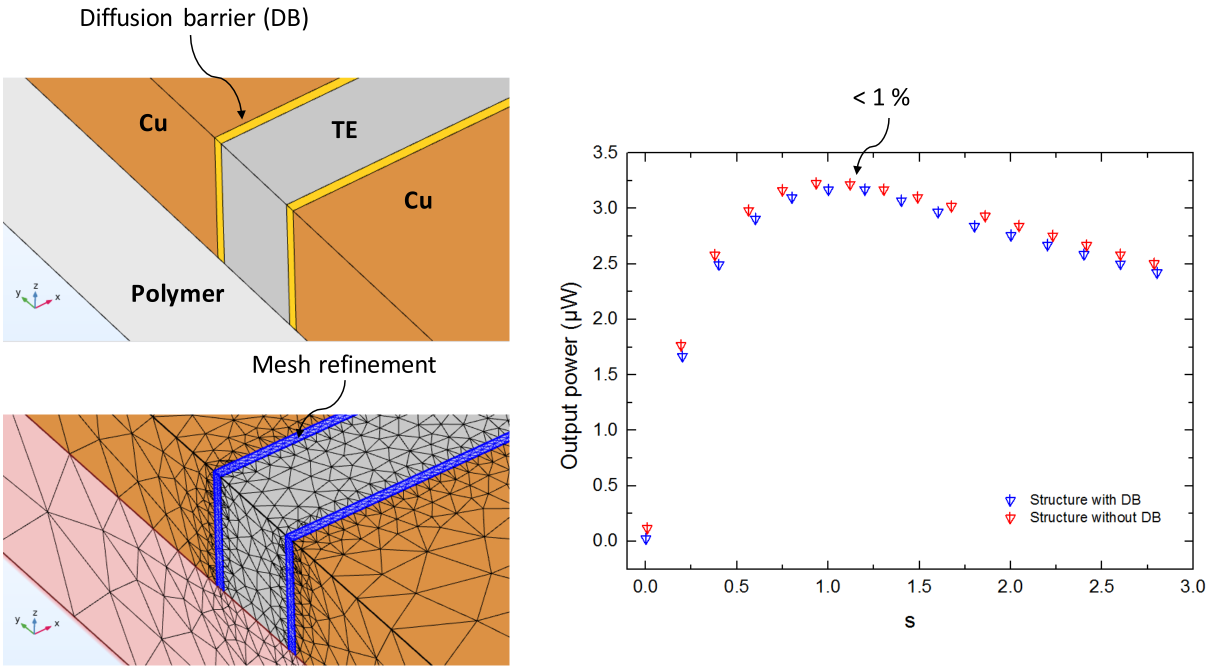

Figure S9. Calculated output power as a function of the parameter $s = R_{load}/R$ for fixed boundary conditions and for $\Delta T = 1$ K with and without the presence of the ENIG diffusion barrier (DB). In these calculations, a thickness of 200 nm has been considered.